Daam2 Driven Degradation of VHL Promotes Gliomagenesis

Wenyi Zhu[1-2], Saritha Krishna[1], Cristina Garcia[1], Chia-Ching John Lin[1], Ken Scott[3], Carrie A Mohila[4], Chad J Creighton[5-6], Seung-Hee Yoo[7], Hyun Kyoung Lee [8-10*], and Benjamin Deneen[1-2,9-10*]

[1] Center for Cell and Gene Therapy, Baylor College of Medicine

[2] The Integrative Molecular and Biomedical Sciences Graduate Program (IMBS), Baylor College of Medicine

[3] Department of Human and Molecular Genetics, Baylor College of Medicine

[4] Department of Pathology, Texas Children's Hospital

[5] Dan L Duncan Cancer Center, Division of Biostatistics, Baylor College of Medicine

[6] Department of Medicine, Baylor College of Medicine

[7] Department of Biochemistry and Molecular Biology, The University of Texas Heath Science Center at Houston

[8] Department of Pediatrics, Division of Neurology, Baylor College of Medicine

[9] Neurological Research Institute, Texas Children's Hospital

[10] Department of Neuroscience, Baylor College of Medicine

Baylor College of Medicine

One Baylor Plaza

Houston, Tx 77030

* Co-corresponding (hyunkyol@bcm.edu and deneen@bcm.edu)

Abstract

Von Hippel-Landau (VHL) protein is a potent tumor suppressor regulating numerous pathways that drive cancer, but mutations in VHL are restricted to limited subsets of malignancies. Here we identified a novel mechanism for VHL suppression in tumors that do not have inactivating mutations. Using developmental processes to uncover new pathways contributing to tumorigenesis, we found that Daam2 promotes glioma formation. Protein expression screening identified an inverse correlation between Daam2 and VHL expression across a host of cancers, including glioma. These *in silico* insights guided corroborating functional studies, which revealed that Daam2 promotes tumorigenesis by suppressing VHL expression. Furthermore, biochemical analyses demonstrate that Daam2 associates with VHL and facilitates its ubiquitination and degradation. Together, these studies are the first to define an upstream mechanism regulating VHL suppression in cancer and describe the role of Daam2 in tumorigenesis.

Key Words

Daam2, Von Hippel Landau protein, Glioblastoma Multiforme, Mouse Glioma Model, Tumorigenesis, Ubiquitination, HIF1α, pAkt.

Running Title: Daam2 suppresses VHL during glioma tumorigenesis

Statement of Significance

We found that the glial developmental factor Daam2 promotes glioma tumorigenesis by suppressing VHL expression. Our studies show, for the first time, a regulatory mechanism that operates upstream of VHL in cancer and provides an explanation for how VHL expression is extinguished in tumors that do not have inactivating mutations.

Introduction

Tumor suppressor and oncogenic pathways function in part by subverting existing cellular programs to promote cancer "hallmark" properties that engender malignant growth (Hanahan and Weinberg, 2011). This corruption of normal cellular physiology is mediated by aberrant activities of these tumorigenic pathways, which are predominantly driven by genetic mutation. Importantly, genetic mutation is not the sole source of this dysregulation, as changes in gene expression via promoter methylation or protein turnover can phenotypically resemble driver mutations and contribute to tumorigenesis (Esteller et al., 1999; Hegi et al., 2004; Pineda et al., 2015; Reinstein and Ciechanover, 2006; Semenza, 2003; Shen et al., 2005; Zochbauer-Muller et al., 2001). While these broad regulatory processes have been linked to cancer, the underlying molecular mechanisms that regulate expression of key components of tumorigenic pathways are very poorly characterized.

VHL is a key tumor suppressor that is mutated in Von Hippel-Landau disease, a hereditary form of clear-cell renal carcinoma (ccRCC) (Chen et al., 1995; Gossage et al., 2015; Kim and Kaelin, 2004; Maher et al., 1990). VHL functions by binding to HIF1α and pAkt and modulating their degradation and activity, respectively. Mutant forms of *VHL* associated with ccRCC are incapable of binding HIF1α or pAkt, resulting in stabilized expression and activation of these proteins, which ultimately facilitates tumorigenesis (Guo et al., 2016; Ivan et al., 2001; Jaakkola et al., 2001; Maxwell et al., 1999; Min et al., 2002; Ohh et al., 2000). While dysregulated HIF1α and pAkt are associated with most forms of

cancer, mutations in VHL are found predominately in ccRCC. This dichotomy suggests that additional regulatory mechanisms oversee VHL dysregulation or inactivation in other malignancies. Indeed recent studies have shown that ID2 can interfere with VHL activity in glioma cell lines (Lee et al., 2016). However, the upstream mechanisms that directly regulate *VHL* expression and protein turnover in cancer remain undefined.

One potential mode of tumor suppressor gene regulation is through developmental mechanisms. Developmental processes directly contribute to all forms of malignancy and are utilized by tumorigenic pathways to maintain cells in an undifferentiated and proliferative state (Jackson et al., 2006; Kesari et al., 2005; Stiles and Rowitch, 2008). Given these established molecular and functional interactions, it stands to reason that expression of tumorigenic pathways may be reciprocally regulated by developmental mechanisms. However, whether such reciprocal regulation of tumor suppressor pathways by developmental factors contributes to tumorigenesis is poorly defined.

To investigate the interface between developmental programs and the regulation of tumor suppressor pathways, we used malignant glioma as a model system. As a molecular entry point for these studies, we focused on Daam2, a key developmental regulator that suppresses glial differentiation and also contributes to dorsal patterning in the developing CNS (Lee et al., 2015; Lee and Deneen, 2012). Here we found that Daam2 promotes tumorigenesis in mouse and human models of malignant glioma. Bioinformatics analysis revealed that Daam2 and VHL expression is inversely correlated across a host of human

123 malignancies. These *in silico* observations are corroborated by *in vivo* functional
124 studies, which revealed that Daam2 promotes tumorigenesis by suppressing
125 VHL expression. Mechanistically, we found that Daam2 associates with VHL and
126 facilitates its degradation by the ubiquitin pathway. Together, these studies
127 represent the initial characterization of Daam2 function in glioma and define, for
128 the first time, an upstream regulatory mechanism that controls VHL protein
129 expression in cancer. Moreover, because mutations in VHL are restricted to a
130 limited set of malignancies, we have identified a new mechanism for VHL
131 inactivation in tumors that do not have inactivating mutations.
132
133 **Results**
134 *Daam2 is expressed in human and mouse glioma*
135 Previously, we identified Daam2 as a component of the Wnt receptor complex
136 that directly contributes to dorsal patterning in the embryonic spinal cord and
137 oligodendrocyte differentiation during development and after injury (Lee et al.,
138 2015; Lee and Deneen, 2012). To further explore its role in neurological diseases,
139 we sought to investigate its role in malignancies of the CNS. Towards this we
140 took advantage of the TCGA pan-cancer expression data set (Akbani et al., 2014;
141 Cancer Genome Atlas Research et al., 2013) and evaluated Daam2 expression
142 across a spectrum of 34 malignancies, finding that it's most highly expressed in
143 low-grade glioma (LGG) and glioblastoma multiforme (GBM) (Figure 1A).
144 To validate Daam2 expression in LGG and GBM, we used in situ
145 hybridization (ISH) across a cohort of 35 LGG and 40 GBM primary human

146 samples, finding that Daam2 demonstrates heterogeneous expression within
147 each glioma sub-type (Fig.1B-C). Notably, the majority of tumors exhibited
148 staining intensity scores that exceeded normal brain samples, indicating that
149 Daam2 expression is elevated within glioma tumors (Fig. 1B-C; Supplemental
150 Figure S1). Next, we evaluated Daam2 expression in our mouse model of
151 malignant glioma, where we combine in utero electroporation (IUE), with
152 CRISPR-mediated deletion of *NFI*, *PTEN*, and *p53* (herein CRISPR/IUE)
153 (Supplemental figure S2) (Chen et al., 2016; Chen and LoTurco, 2012; Chen et
154 al., 2012; Cong et al., 2013; John Lin et al., 2017b). This model closely
155 resembles the genetics of GBM (Alcantara Llaguno et al., 2009; Kwon et al.,
156 2008; Zhu et al., 2005) and begins producing tumors detectable around post-
157 natal week 8. Combining this model, with our the Daam2-LacZ mouse line, we
158 performed immunostaining on the resultant tumors, finding that Daam2 exhibits
159 elevated expression levels in tumors, compared to normal brain tissue (Figure
160 1D). Finally, we evaluated Daam2 expression in xenograft tumors generated
161 from primary human GBM cell lines, finding that Daam2 is also highly expressed
162 in these human cell line models (Supplemental Figure S1). Put together, these
163 studies indicate that Daam2 expression is elevated in both human LGG and
164 GBM and is expressed in the associated model systems.
165
166 *Overexpression of Daam2 accelerates glioma tumorigenesis*
167 The forging expression analysis in human glioma and associated mouse models
168 led us to examine whether Daam2 contributes to glioma tumorigenesis. To

assess its role in glioma, we performed overexpression, gain-of-function (GOF) studies in human GBM cell lines, finding that Daam2 accelerates the rate of cell growth *in vitro* (Figure 2A-B). Next, we determined how Daam2 influences anchorage independent growth, via soft agar assay, finding that it also accelerates colony formation (Figure 2C-D). Together, these *in vitro* studies, indicate that Daam2 promotes cell proliferation and growth in human GBM cell lines

To evaluate the role of Daam2 in tumorigenesis, we turned to mouse models of malignant glioma. The first model combines targeted PiggyBac overexpression of oncogenic Ras-V12 (PB-Ras) in glial precursors with IUE, to generate malignant glioma in mice around post-natal day 14 (Supplemental Figure S2). Combining PiggyBac-mediated overexpression of Daam2 with this Ras-driven model resulted in an acceleration of tumorigenesis (Supplemental Figure S3). To further substantiate these findings in additional mouse models, we next used our CRISPR/IUE model (Supplemental Figure S2). Consistent with the Ras model, combined overexpression of Daam2 in the CRISPR/IUE model, also resulted in accelerated tumorigenesis (Figure 2E-G). BrdU labeling analysis of the resulting tumors from both models revealed that overexpression of Daam2 results in an increase in the number BrdU-expressing cells (Figure 2H-J; Supplemental Figure S3). These data, combined with our *in vitro* studies, indicate that overexpression of Daam2 promotes glioma cell proliferation and tumorigenesis.

Loss of Daam2 impairs glioma tumorigenesis

To further delineate the role of Daam2 in glioma, we next performed a series of complementary loss-of-function (LOF) studies in human and mouse glioma models. In human GBM cell lines we performed shRNAi-mediated knockdown of human Daam2, finding that decreased expression of Daam2 inhibited their rate of growth *in vitro* (Figure 3A-B). Next, we assessed the tumorigenic potential of these GBM cell lines, finding that knockdown of Daam2 resulted in a significant decrease in tumor growth *in vivo* (Figure 3C-E). These knockdown studies across both *in vitro* and *in vivo* systems, complement the overexpression studies, and further substantiate the role of Daam2 in glioma cell proliferation and tumorigenesis.

To further evaluate the necessity for Daam2 in glioma tumorigenesis, we used CRISPR/IUE model to generate malignant glioma in *Daam2*$^{+/-}$ and *Daam2*$^{-/-}$ mice (Lee et al., 2015). As shown in Figure 3F-H, mice lacking Daam2 demonstrated decreased rates of tumor formation in this model compared to the heterozygote control. Moreover, BrdU labeling revealed substantial decreases in the number of proliferating cells in *Daam2*$^{-/-}$ tumors (Figure 3I-K). Together, our LOF, and complementing GOF (Figure 2) studies in human and mouse models of glioma indicate that Daam2 promotes cell proliferation and tumorigenesis.

Daam2 suppresses VHL expression

Having established that Daam2 functions to promote glioma tumorigenesis, we next sought to uncover the mechanism by which it operates. Previously, we

found that Daam2 functions as a positive regulator of Wnt-signaling in the developing CNS (Lee and Deneen, 2012), suggesting that it may also function in this manner in glioma. To evaluate Wnt-activity we used an established Wnt-reporter (TOP-FLASH) and found that modulation of Daam2 expression has a modest effect on Wnt activity in glioma cell lines and did not impact Wnt activity in our mouse model of glioma (Supplemental Figure S4).

That Wnt-activity is not affected by changes in Daam2 expression raises the question of how Daam2 promotes glioma tumorigenesis. To identify changes in protein expression associated with Daam2-mediated tumorigenesis we performed reverse phase protein lysate microarray (RPPA) on FACS-isolated mouse glioma samples that overexpress Daam2. Analysis revealed a cohort of proteins that are strongly downregulated in glioma samples that overexpress Daam2 (Figure 4A; Supplemental Figure S4; Supplemental Table I). To further substantiate these potential relationships, we leveraged existing TCGA RNA-Seq and RPPA data to determine whether there is an inverse correlation between Daam2 expression and this cohort of proteins across a spectrum of human malignancies (Supplemental Figure S5). This analysis identified Von Hippel Landau (VHL) as one of the proteins from this cohort with the most significant inverse correlation score across this spectrum of malignancies, with lung adenocarcinoma and GBM demonstrating the strongest negative correlations between Daam2 and VHL (Figure 4B; Supplemental Figure S5).

VHL is an established tumor suppressor that is frequently mutated in clear cell renal carcinoma (ccRCC) and functions by facilitating the degradation of

238 HIF1α and pAkt (Guo et al., 2016; Ivan et al., 2001; Jaakkola et al., 2001;
239 Maxwell et al., 1999; Min et al., 2002; Ohh et al., 2000). Given that Daam2
240 expression is inversely correlated with VHL, we next assessed whether Daam2
241 demonstrates congruent correlation with HIF1α and pAkt in the panel of human
242 cancers. Analysis of these data revealed that Daam2 expression was positively
243 correlated with HIF1α and pAkt protein expression across this cohort of
244 malignancies, with GBM and lung adenocarcinoma also showing the strongest
245 positive correlation (Figure 4B). Together, our RPPA screen and associated
246 bioinformatics analysis of human malignancies indicate that Daam2 expression is
247 inversely correlated with VHL expression and positively correlated with its
248 downstream signaling axis.
249
250 *Daam2 promotes tumorigenesis through VHL*
251 The RPPA data suggests that Daam2 modulates expression of VHL in glioma.
252 To directly test this hypothesis, we evaluated expression of VHL and its signaling
253 axis in our Daam2-GOF and Daam2-LOF mouse tumor models. Immunostaining
254 for VHL in these models corroborated our RPPA data, where VHL expression
255 was dramatically reduced in Daam2-GOF tumors, and increased in the *Daam2*$^{-/-}$
256 tumors (Figure 4C-F). Next we assessed expression of VHL's downstream
257 effectors, pAkt and HIF1α, finding that both of these proteins demonstrated
258 elevated levels of expression in the Daam2-GOF tumors, and pAkt having
259 decreased levels in the *Daam2*$^{-/-}$ tumors (Figure 4G-K). One consequence of
260 elevated HIF1α is increased angiogenesis (Fan et al., 2014; Keith and Simon,

2007; Semenza, 2004), which we detected in Daam2-GOF tumors via staining for the endothelial marker, CD31 (Supplemental Figure S6). These data, combined with our bioinformatics analysis, indicate that Daam2 suppresses VHL-signaling in malignant glioma.

These observations raise the question of whether the effects of Daam2 on glioma tumorigenesis are mediated through its suppression of VHL expression. To determine whether an epistatic relationship exists, we overexpressed VHL in the presence of Daam2 overexpression in human GBM cell lines, finding that VHL suppresses the increased rate of cell growth mediated by Daam2-alone (Figure 5A-B). Next, we extended these studies to our mouse models of glioma, finding that combined overexpression of VHL with Daam2 similarly suppressed the accelerated rate of tumorigenesis and proliferation mediated by Daam2-alone (Figure 5C-I). Moreover, overexpression of VHL resulted in concordant suppression of pAkt and angiogenesis in these tumors (Figure 5J-P; Supplemental Figure S6). Put together, these data indicate that Daam2 promotes tumorigenesis by suppressing VHL expression in glioma.

Daam2 facilitates ubiquitination of VHL protein

Analysis of human cancer data, along with our functional studies in mouse models, strongly suggests that Daam2 expression results in the loss of VHL protein. To determine the mechanism by which Daam2 influences the levels of VHL protein, we next performed a series of immunoprecipitation experiments to evaluate the biochemical relationship between Daam2 and VHL. Using protein

lysates extracted from our PB-Ras model of glioma, we found that Daam2 co-immunoprecipitates with VHL, suggesting that these proteins associate (Figure 6A).

Given that Daam2 associates with VHL, and expression of VHL protein is negatively correlated with Daam2, we hypothesized that these expression dynamics are the result of Daam2 promoting the degradation of VHL. To test this we co-transfected Daam2 and VHL in 293 cells, and measured the rate of cyclohexamide-mediated degradation, finding that VHL degradation is significantly enhanced in the presence of Daam2 (Figure 6B, D). The ubiquitination pathway is a central mechanism that oversees protein degradation, (Pickart and Eddins, 2004) (Kerscher et al., 2006; Ulrich and Walden, 2010), therefore, we next examined whether Daam2 facilitates the ubiquitintion of VHL. Using *in vitro* systems, we found that in the presence of elevated levels of Daam2, the extent of VHL ubiquitination is substantially increased and levels of VHL protein demonstrate a concomitantly decrease (Figure 6C). Together, these mechanistic studies reveal that the underlying biochemical relationship between Daam2 and VHL is mediated by ubiquitin-driven protein degradation.

Discussion

Using factors critical for central nervous system (CNS) development as an entry point to identify new mechanisms that contribute to tumorigenesis, we found that the glial development factor, Daam2 promotes glioma tumorigenesis across human glioma cell lines and multiple mouse models of glioma. Protein screening

and bioinformatics studies revealed that Daam2 and VHL expression is inversely correlated across a broad spectrum of cancers, while functional interrogation of this relationship demonstrated that Daam2 promotes tumorigenesis via suppression of VHL expression. Mechanistically, Daam2 associates with VHL and stimulates its ubiquitination and degradation. Together, these studies are the first to define an upstream mechanism regulating VHL protein turnover in cancer and describe the role of Daam2 in tumorigenesis.

Daam2 stimulates glioma tumorigenesis

Leveraging existing TCGA expression data across a broad spectrum of malignancies, we found that Daam2 is most highly expressed in glioma and melanoma. These expression characteristics in glioma were confirmed using tissue arrays and functional studies revealed that Daam2 promotes cell proliferation and tumorigenesis in human and mouse glioma models. These are the first studies to describe the role of Daam-family proteins in tumorigenesis. Daam1 and Daam2 have highly conserved formin domains yet exhibit non-overlapping expression patterns in the developing CNS (Habas et al., 2001; Kida et al., 2004; Lee and Deneen, 2012; Nakaya et al., 2004), suggesting distinct functions during development. Indeed, Daam2 functions in this context via canonical Wnt-signaling, while Daam1 operates via the non-canonical Wnt, planar cell polarity (PCP) pathway (Habas et al., 2001; Lee and Deneen, 2012; Li et al., 2011; Liu et al., 2008; Zhu et al., 2012). It will be important to discern whether this functional diversity between Daam1 and Daam2 is also applicable to

CNS malignancies. Given that the PCP pathway has been implicated in tumor cell invasion and migration (Anastas and Moon, 2013; Paw et al., 2015; Weeraratna et al., 2002), it is possible that Daam-family proteins also contribute to these features of tumorigenesis. Recent studies have implicated Daam1, Daam2 and other formin-family genes in the migration of breast and neuroblastoma cell lines (Luga et al., 2012), respectively, suggesting that the Daam-family proteins may also contribute to invasion and metastasis in other malignancies.

Our previous studies have shown that Daam2 potentiates canonical Wnt signaling through the clustering of existing Wnt receptor complexes (Lee and Deneen, 2012). While the Wnt pathway has been implicated in several forms of cancer, including medulloblastoma, mutations in key components of the Wnt-pathway and dysregulated Wnt-signaling has not been widely linked to low- or high-grade glioma (Bienz and Clevers, 2000; de La Coste et al., 1998; Klaus and Birchmeier, 2008; Lustig and Behrens, 2003; Morin et al., 1997; Rubinfeld et al., 1997; Zurawel et al., 1998). This, coupled with the fact that Daam2 acts upon existing Wnt receptor complexes, may explain why we did not witness any overt changes in Wnt activity when we manipulated Daam2 expression in our glioma models. Nevertheless, we cannot formally rule out a possible role for Daam2 in canonical or non-canonical Wnt signaling in glioma or in other malignancies driven by Wnt dysregulation.

353 *New Parallels Between Development and Cancer*

354 Our observation that manipulation of Daam2 expression promoted tumorigenesis,
355 but not canonical Wnt signaling, points to the possibility that it functions through a
356 Wnt-independent mechanism. RPPA and bioinformatics approaches revealed
357 that Daam2 expression is inversely correlated with a cohort of genes (Figure S5),
358 including VHL, across a broad spectrum of cancers. Moreover, the RPPA data
359 analysis identified a larger cohort of proteins that were downregulated in the
360 presence of Daam2 in our mouse model of glioma. These observations, coupled
361 with our findings that Daam2 associates with- and facilitates- the ubiquitination of
362 VHL, suggest that it may also play a role in the ubiquitination pathway. The
363 nature of this prospective relationship between Daam2 and the existing
364 ubiquitination machinery, and whether these relationships are specific to
365 malignancy or can be extended to development are areas of future investigation
366 and represent potentially new parallels between development and cancer. Indeed
367 dysregulation of ubiquitination is linked to protein aggregation associated with
368 several neurological disorders, functioning through both neuronal and glial
369 populations (Jansen, et al. 2014 and Hedge and Upadhya, 2007)

370 Another feature of Daam2 is that it functions to suppress the differentiation
371 of oligodendrocyte progenitor cells (OPC) during development and after injury
372 (Lee et al., 2015). Studies in mouse models suggest that OPCs may serve as a
373 cell of origin for glioma, while NG2-positive OPC populations are endowed with
374 tumor initiating properties (Ligon et al., 2007; Liu et al., 2011; Persson et al.,
375 2010; Stiles and Rowitch, 2008; Sugiarto et al., 2011; Yadavilli et al., 2015).

Moreover, OPCs have latent proliferative capacity that is essential for injury responses, suggesting parallels between the processes that drive injury responses and tumorigenesis. Indeed recent studies have linked the VHL-HIF1α signaling axis to OPC development and neonatal hypoxic injury responses (Yuen et al., 2014). That Daam2 promotes tumorigenesis via suppression of VHL and also regulates OPC development and injury responses, suggests that it may also utilize these tumorigenic mechanisms in the context of injury. Together these findings add to the emerging evidence that OPC associated signaling networks play critical roles in glioma pathophysiology and further reinforce the parallels between neurological disorders and cancer biology.

Regulation of VHL in cancer

Mechanistic studies revealed that Daam2 promotes glioma tumorigenesis via suppression of VHL, a classic tumor suppressor that promotes HIF1α degradation and inhibits Akt activity. Importantly, inactivating mutations in VHL are predominately found in ccRCC and are very rare in most other forms of cancer, including glioma. These observations raise the critical question of how HIF1α becomes upregulated in cancers that do not exhibit VHL mutations. Our studies show, for the first time, a regulatory mechanism that operates upstream of VHL in cancer and provides an explanation for how VHL expression is extinguished in tumors that do not have inactivating mutations. Moreover, because Daam2-VHL expression demonstrates a robust, inverse correlation across a spectrum of cancers, this is likely to be a generalized mechanism of

VHL suppression in cancer. Interestingly, prior studies in yeast have shown that VHL can be degraded via the Hsp70 and Hsp110 chaperone system (McClellan et al., 2005; Melville et al., 2003). Given that Hsp's are expressed across a host of cancers (Garcia-Morales et al., 2007; Nylandsted et al., 2002; Sauvageot et al., 2009), it will be important to determine whether Daam2 engages the Hsp chaperone system to facilitate VHL degradation in glioma and other malignancies.

Given its role as the central regulator of HIF1α, surprisingly little is known about the regulatory biology surrounding VHL and its role in glioma formation. Studies in glioma cell lines suggest that ID2 interference with VHL activity can deregulate HIF1α expression and promote tumorigenesis in xenograft models (Lee et al., 2016). Interestingly, ID2 has also been linked to the suppression of OPC differentiation via direct regulation of cell cycle kinetics (Wang et al., 2001). These observations further reinforce the relationship between OPC development and glioma tumorigenesis and highlight key parallels between ID2 and Daam2 function across these systems, as both genes suppress VHL, inhibit OPC differentiation, and promote glioma tumorigenesis. Because both proteins associated with- and regulate- VHL, albeit via distinct mechanisms, it's possible that these suppressive functions are coordinated and contribute tumorigenesis. From this, a model emerges where ID2 displaces VHL from the ubiquitin complex, which facilitates its association with Daam2 and its subsequent ubiquitination and degradation. It will be important to decipher whether ID2 and Daam2 functions are in fact coordinated, and the extent to which Hsp proteins participate in this mechanism. Finally, understanding whether and how these prospective

422 relationships are also applicable to OPC development and injury responses may
423 also reveal new insights in CNS repair mechanisms.
424
425 **Materials and Methods**
426 **TCGA database analysis and Comparative Bioinformatics**
427 RNA expression data underlying the results presented in Figure 1 were
428 generated by TCGA Research Network (http://cancergenome.nih.gov/). All data
429 used in this study were publicly available, e.g. from The Broad Institute's
430 Firehose pipeline (http://gdac.broadinstitute.org/). From TCGA, we collected
431 molecular data on 10224 tumors of various histological subtypes, for which RNA-
432 seq data (v2 platform alignment) were available. Correlation between VHL and
433 AKT pS473 protein on TCGA samples, were obtained from The Cancer
434 Proteome Atlas, or TCPA.
435
436 **In Utero Electroporation (IUE)**
437 To generate mouse gliomas, we performed in utero electroporation (IUE). Briefly,
438 the uterine horns were exposed, and DNA combination was injected into the
439 embryonic lateral ventricles along with Fast Green dye as the indicator. Then
440 electroporation was accomplished by BTW tweezertrodes connected with the
441 pulse generator (BTX 8300) in the setting of 33V, 55ms per pulse100ms intervals.
442 In CRISPR-IUE model, the DNA combination is composed of the "helper-plasmid"
443 pGLAST-PBase (2.0 ug/ul) and all the other DNA (1.0 ug/ul), including pbCAG-
444 GFP, pbCAG-Luciferase, crNF1, crPTEN, crp53(Chen and LoTurco, 2012; John

445 Lin et al., 2017a). In the HRas-IUE model, the DNA combination is composed of
446 pGLAST-PBase (2.0 ug/ul) and others (1.0 ug/ul), including pbCAG-GFP2aHRas
447 and pbCAG-Luciferase.
448
449 **Glioma Xenograft Assays**
450 6-week-old SCID male mice (Taconic) were used for human GBM cell line
451 transplantation. $4x10^4$ luciferase-infected primary GBM cells were injected into
452 each mouse brain, at the location of the 1mm front, 2mm right, 3mm deep from
453 the Bregma. Animals were euthanized and perfused six weeks after
454 transplantation of GBM cells. Brains were fixed in 4% paraformaldehyde and
455 70% EtOH overnight, respectively. After fixation, brains were embedded in
456 paraffin, sectioned and subjected to molecular and pathological analysis via
457 immunostaining or hematoxylin and eosin staining.
458
459 **Bioluminescent Imaging**
460 To measure the tumor growth after manipulation of Daam2 we performed
461 bioluminescent imaging before harvesting. Mice were monitored once a week. D-
462 Luciferin (Perkin Elmer, #122799) was diluted to 15 mg/ml with PBS and injected
463 into each mouse at a dose of 10 ul/g body weight.
464
465 **Cell Growth Curve and Agar Assays**
466 For *in vitro* human GBM cell line studies, adult GBM-1 and GBM-2 cell lines were
467 kindly provided from Dr. Nabil Ahmed (Hegde et al., 2013). To manipulate the

468 expression of Daam2 in GBM cell lines, we used the lentivirus as described
469 above. To virally infect human primary GBM cells, $1.5x10^4$ cells were plated in 6-
470 well plates with DMEM + 10% FBS. Cells were infected with either Daam2 or
471 Daam2 shRNAi virus for 14 hours to make the stable cell line for GOF and LOF
472 study, respectively. To assess rates of cell growth, $2x10^4$ cells were plated in 12-
473 well plates and cells were counted over the course of three days.
474 For the agar assay, $2.5x10^4$ cells (cell agar layer) was mixed with 5ml
475 Iscove's 1.4% Nobel Agar + 40% FBS, covered by top and bottom coating agar
476 layers (2ml Iscove's 1.4% Nobel Agar + 20% FBS) in a 6mm plate. We tightly
477 monitored the colony formation for several weeks.
478
479 **In Vitro Degradation Assay**
480 To test VHL degradation, 1×10^5 293T cells were plated into the 12 well plate
481 one day before transfection. 100 ng Myc-tagged Daam2 and GFP-tagged VHL
482 was transfected by iMFectin DNA Transfection Reagent (GenDEPOT) according
483 to the protocol. 30 hours post-transfection, cells were treated with 50 ul/ml CHX
484 for 0, 2, 4, 6 ,hours. Lysis and Western blot process is described in the
485 supplemental methods. To quantify the protein abundance the Western blot band
486 intensity in the 0-hour sample of both VHL+/- Damm2 groups are set as "1". The
487 intensity of 2, 4, 6-hour degradation western blot band is normalized and plotted
488 using Nonlinear Regression Curve by GraphPad.
489
490 **Statistical Analysis**

One-way ANOVA was used to analyze bioluminescent intensity and BrdU-positive cell counts to determine the differences between Ctrl, D2 and D2/VHL groups, followed by Tukey's test to compare between individual groups, which is demarcated by an asterisk in the graphs. Independent *t*-test was used to analyze the differences in bioluminescent intensity and BrdU-positive cell counts between Ctrl vs. D2, Het vs. KO, Scrambled-shRNAi vs. D2-shRNAi.

Please see supplemental methods for additional experimental details.

Author Contributions

Conceptualization: W.Z, H.K.L, and B.D.; Methodology: W.Z., S.K., C.G., C.C.L., C.A.M., S.H.Y., H.K.L; Data Analysis: W.Z., C.J.C, C.A.M., H.K.L., B.D.; Key Reagents: K.S., S.H.Y; Writing Manuscript: W.Z., H.K.L, and B.D.

Acknowledgements

This work was supported by grants from the Sontag Foundation (BD), Cancer Prevention Research Institute of Texas (RP510334 and RP160192 to BD and CC), and the National Institutes of Health (NS071153 and NS089366 to BD). National Multiple Sclerosis Scoiety (TA3054-A to HKL). We acknowledge the assistance of the Baylor College of Medicine Mouse Phenotyping Core, the Lester and Sue Smith Breast Center's Pathology Core, and Functional Proteomics RPPA Core Facility at MD Anderson Cancer Center, this facility is funded by NCI # CA16672. This project was also supported in part by the IDDRC

grant number 1U54 HD083092 from the Eunice Kennedy Shriver National Institute of Child Health & Human Development.

References

Akbani, R., Ng, P.K., Werner, H.M., Shahmoradgoli, M., Zhang, F., Ju, Z., Liu, W., Yang, J.Y., Yoshihara, K., Li, J.*, et al.* (2014). A pan-cancer proteomic perspective on The Cancer Genome Atlas. Nat Commun *5*, 3887.

Alcantara Llaguno, S., Chen, J., Kwon, C.H., Jackson, E.L., Li, Y., Burns, D.K., Alvarez-Buylla, A., and Parada, L.F. (2009). Malignant astrocytomas originate from neural stem/progenitor cells in a somatic tumor suppressor mouse model. Cancer Cell *15*, 45-56.

Anastas, J.N., and Moon, R.T. (2013). WNT signalling pathways as therapeutic targets in cancer. Nat Rev Cancer *13*, 11-26.

Bienz, M., and Clevers, H. (2000). Linking colorectal cancer to Wnt signaling. Cell *103*, 311-320.

Cancer Genome Atlas Research, N., Weinstein, J.N., Collisson, E.A., Mills, G.B., Shaw, K.R., Ozenberger, B.A., Ellrott, K., Shmulevich, I., Sander, C., and Stuart, J.M. (2013). The Cancer Genome Atlas Pan-Cancer analysis project. Nat Genet *45*, 1113-1120.

Chen, F., Becker, A., and LoTurco, J. (2016). Overview of Transgenic Glioblastoma and Oligoastrocytoma CNS Models and Their Utility in Drug Discovery. Curr Protoc Pharmacol *72*, 14 37 11-12.

Chen, F., Kishida, T., Yao, M., Hustad, T., Glavac, D., Dean, M., Gnarra, J.R., Orcutt, M.L., Duh, F.M., Glenn, G.*, et al.* (1995). Germline mutations in the von Hippel-Lindau disease tumor suppressor gene: correlations with phenotype. Hum Mutat *5*, 66-75.

Chen, F., and LoTurco, J. (2012). A method for stable transgenesis of radial glia lineage in rat neocortex by piggyBac mediated transposition. J Neurosci Methods *207*, 172-180.

Chen, J., Li, Y., Yu, T.S., McKay, R.M., Burns, D.K., Kernie, S.G., and Parada, L.F. (2012). A restricted cell population propagates glioblastoma growth after chemotherapy. Nature *488*, 522-526.

Cong, L., Ran, F.A., Cox, D., Lin, S., Barretto, R., Habib, N., Hsu, P.D., Wu, X., Jiang, W., Marraffini, L.A.*, et al.* (2013). Multiplex genome engineering using CRISPR/Cas systems. Science *339*, 819-823.

de La Coste, A., Romagnolo, B., Billuart, P., Renard, C.A., Buendia, M.A., Soubrane, O., Fabre, M., Chelly, J., Beldjord, C., Kahn, A., *et al.* (1998). Somatic mutations of the beta-catenin gene are frequent in mouse and human hepatocellular carcinomas. Proc Natl Acad Sci U S A *95*, 8847-8851.

Esteller, M., Hamilton, S.R., Burger, P.C., Baylin, S.B., and Herman, J.G. (1999). Inactivation of the DNA repair gene O6-methylguanine-DNA methyltransferase by promoter hypermethylation is a common event in primary human neoplasia. Cancer Res *59*, 793-797.

Fan, Y., Potdar, A.A., Gong, Y., Eswarappa, S.M., Donnola, S., Lathia, J.D., Hambardzumyan, D., Rich, J.N., and Fox, P.L. (2014). Profilin-1 phosphorylation directs angiocrine expression and glioblastoma progression through HIF-1alpha accumulation. Nat Cell Biol *16*, 445-456.

Garcia-Morales, P., Carrasco-Garcia, E., Ruiz-Rico, P., Martinez-Mira, R., Menendez-Gutierrez, M.P., Ferragut, J.A., Saceda, M., and Martinez-Lacaci, I. (2007). Inhibition of Hsp90 function by ansamycins causes downregulation of cdc2 and cdc25c and G(2)/M arrest in glioblastoma cell lines. Oncogene *26*, 7185-7193.

Gossage, L., Eisen, T., and Maher, E.R. (2015). VHL, the story of a tumour suppressor gene. Nat Rev Cancer *15*, 55-64.

Guo, J., Chakraborty, A.A., Liu, P., Gan, W., Zheng, X., Inuzuka, H., Wang, B., Zhang, J., Zhang, L., Yuan, M., *et al.* (2016). pVHL suppresses kinase activity of Akt in a proline-hydroxylation-dependent manner. Science *353*, 929-932.

Habas, R., Kato, Y., and He, X. (2001). Wnt/Frizzled activation of Rho regulates vertebrate gastrulation and requires a novel Formin homology protein Daam1. Cell *107*, 843-854.

Hanahan, D., and Weinberg, R.A. (2011). Hallmarks of cancer: the next generation. Cell *144*, 646-674.

Hegde, M., Corder, A., Chow, K.K., Mukherjee, M., Ashoori, A., Kew, Y., Zhang, Y.J., Baskin, D.S., Merchant, F.A., Brawley, V.S., *et al.* (2013). Combinational Targeting Offsets Antigen Escape and Enhances Effector Functions of Adoptively Transferred T Cells in Glioblastoma. Mol Ther *21*, 2087-2101.

Hegi, M.E., Diserens, A.C., Godard, S., Dietrich, P.Y., Regli, L., Ostermann, S., Otten, P., Van Melle, G., de Tribolet, N., and Stupp, R. (2004). Clinical trial substantiates the predictive value of O-6-methylguanine-DNA methyltransferase promoter methylation in glioblastoma patients treated with temozolomide. Clin Cancer Res *10*, 1871-1874.

Ivan, M., Kondo, K., Yang, H., Kim, W., Valiando, J., Ohh, M., Salic, A., Asara, J.M., Lane, W.S., and Kaelin, W.G., Jr. (2001). HIFalpha targeted for VHL-

588 mediated destruction by proline hydroxylation: implications for O2 sensing.
589 Science *292*, 464-468.

590 Jaakkola, P., Mole, D.R., Tian, Y.M., Wilson, M.I., Gielbert, J., Gaskell, S.J., von
591 Kriegsheim, A., Hebestreit, H.F., Mukherji, M., Schofield, C.J., *et al.* (2001).
592 Targeting of HIF-alpha to the von Hippel-Lindau ubiquitylation complex by O2-
593 regulated prolyl hydroxylation. Science *292*, 468-472.

594 Jackson, E.L., Garcia-Verdugo, J.M., Gil-Perotin, S., Roy, M., Quinones-Hinojosa,
595 A., VandenBerg, S., and Alvarez-Buylla, A. (2006). PDGFR alpha-positive B cells
596 are neural stem cells in the adult SVZ that form glioma-like growths in response
597 to increased PDGF signaling. Neuron *51*, 187-199.

598 John Lin, C.C., Yu, K., Hatcher, A., Huang, T.W., Lee, H.K., Carlson, J., Weston,
599 M.C., Chen, F., Zhang, Y., Zhu, W., *et al.* (2017a). Identification of diverse
600 astrocyte populations and their malignant analogs. Nat Neurosci.

601 John Lin, C.C., Yu, K., Hatcher, A., Huang, T.W., Lee, H.K., Carlson, J., Weston,
602 M.C., Chen, F., Zhang, Y., Zhu, W., *et al.* (2017b). Identification of diverse
603 astrocyte populations and their malignant analogs. Nat Neurosci *20*, 396-405.

604 Keith, B., and Simon, M.C. (2007). Hypoxia-inducible factors, stem cells, and
605 cancer. Cell *129*, 465-472.

606 Kerscher, O., Felberbaum, R., and Hochstrasser, M. (2006). Modification of
607 proteins by ubiquitin and ubiquitin-like proteins. Annu Rev Cell Dev Biol *22*, 159-
608 180.

609 Kesari, S., Ramakrishna, N., Sauvageot, C., Stiles, C.D., and Wen, P.Y. (2005).
610 Targeted molecular therapy of malignant gliomas. Curr Neurol Neurosci Rep *5*,
611 186-197.

612 Kida, Y., Shiraishi, T., and Ogura, T. (2004). Identification of chick and mouse
613 Daam1 and Daam2 genes and their expression patterns in the central nervous
614 system. Brain Res Dev Brain Res *153*, 143-150.

615 Kim, W.Y., and Kaelin, W.G. (2004). Role of VHL gene mutation in human cancer.
616 J Clin Oncol *22*, 4991-5004.

617 Klaus, A., and Birchmeier, W. (2008). Wnt signalling and its impact on
618 development and cancer. Nat Rev Cancer *8*, 387-398.

619 Kwon, C.H., Zhao, D., Chen, J., Alcantara, S., Li, Y., Burns, D.K., Mason, R.P.,
620 Lee, E.Y., Wu, H., and Parada, L.F. (2008). Pten haploinsufficiency accelerates
621 formation of high-grade astrocytomas. Cancer Res *68*, 3286-3294.

622 Lee, H.K., Chaboub, L.S., Zhu, W., Zollinger, D., Rasband, M.N., Fancy, S.P.,
623 and Deneen, B. (2015). Daam2-PIP5K is a regulatory pathway for Wnt signaling
624 and therapeutic target for remyelination in the CNS. Neuron *85*, 1227-1243.

625 Lee, H.K., and Deneen, B. (2012). Daam2 is required for dorsal patterning via
626 modulation of canonical Wnt signaling in the developing spinal cord. Dev Cell *22*,
627 183-196.

628 Lee, S.B., Frattini, V., Bansal, M., Castano, A.M., Sherman, D., Hutchinson, K.,
629 Bruce, J.N., Califano, A., Liu, G., Cardozo, T.*, et al.* (2016). An ID2-dependent
630 mechanism for VHL inactivation in cancer. Nature *529*, 172-177.

631 Li, D., Hallett, M.A., Zhu, W., Rubart, M., Liu, Y., Yang, Z., Chen, H., Haneline,
632 L.S., Chan, R.J., Schwartz, R.J.*, et al.* (2011). Dishevelled-associated activator of
633 morphogenesis 1 (Daam1) is required for heart morphogenesis. Development
634 *138*, 303-315.

635 Ligon, K.L., Huillard, E., Mehta, S., Kesari, S., Liu, H., Alberta, J.A., Bachoo,
636 R.M., Kane, M., Louis, D.N., Depinho, R.A.*, et al.* (2007). Olig2-regulated
637 lineage-restricted pathway controls replication competence in neural stem cells
638 and malignant glioma. Neuron *53*, 503-517.

639 Liu, C., Sage, J.C., Miller, M.R., Verhaak, R.G., Hippenmeyer, S., Vogel, H.,
640 Foreman, O., Bronson, R.T., Nishiyama, A., Luo, L.*, et al.* (2011). Mosaic
641 analysis with double markers reveals tumor cell of origin in glioma. Cell *146*, 209-
642 221.

643 Liu, W., Sato, A., Khadka, D., Bharti, R., Diaz, H., Runnels, L.W., and Habas, R.
644 (2008). Mechanism of activation of the Formin protein Daam1. Proc Natl Acad
645 Sci U S A *105*, 210-215.

646 Luga, V., Zhang, L., Viloria-Petit, A.M., Ogunjimi, A.A., Inanlou, M.R., Chiu, E.,
647 Buchanan, M., Hosein, A.N., Basik, M., and Wrana, J.L. (2012). Exosomes
648 mediate stromal mobilization of autocrine Wnt-PCP signaling in breast cancer
649 cell migration. Cell *151*, 1542-1556.

650 Lustig, B., and Behrens, J. (2003). The Wnt signaling pathway and its role in
651 tumor development. J Cancer Res Clin Oncol *129*, 199-221.

652 Maher, E.R., Yates, J.R., Harries, R., Benjamin, C., Harris, R., Moore, A.T., and
653 Ferguson-Smith, M.A. (1990). Clinical features and natural history of von Hippel-
654 Lindau disease. Q J Med *77*, 1151-1163.

655 Maxwell, P.H., Wiesener, M.S., Chang, G.W., Clifford, S.C., Vaux, E.C.,
656 Cockman, M.E., Wykoff, C.C., Pugh, C.W., Maher, E.R., and Ratcliffe, P.J.
657 (1999). The tumour suppressor protein VHL targets hypoxia-inducible factors for
658 oxygen-dependent proteolysis. Nature *399*, 271-275.

McClellan, A.J., Scott, M.D., and Frydman, J. (2005). Folding and quality control of the VHL tumor suppressor proceed through distinct chaperone pathways. Cell *121*, 739-748.

Melville, M.W., McClellan, A.J., Meyer, A.S., Darveau, A., and Frydman, J. (2003). The Hsp70 and TRiC/CCT chaperone systems cooperate in vivo to assemble the von Hippel-Lindau tumor suppressor complex. Mol Cell Biol *23*, 3141-3151.

Min, J.H., Yang, H., Ivan, M., Gertler, F., Kaelin, W.G., Jr., and Pavletich, N.P. (2002). Structure of an HIF-1alpha -pVHL complex: hydroxyproline recognition in signaling. Science *296*, 1886-1889.

Morin, P.J., Sparks, A.B., Korinek, V., Barker, N., Clevers, H., Vogelstein, B., and Kinzler, K.W. (1997). Activation of beta-catenin-Tcf signaling in colon cancer by mutations in beta-catenin or APC. Science *275*, 1787-1790.

Nakaya, M.A., Habas, R., Biris, K., Dunty, W.C., Jr., Kato, Y., He, X., and Yamaguchi, T.P. (2004). Identification and comparative expression analyses of Daam genes in mouse and Xenopus. Gene Expr Patterns *5*, 97-105.

Nylandsted, J., Wick, W., Hirt, U.A., Brand, K., Rohde, M., Leist, M., Weller, M., and Jaattela, M. (2002). Eradication of glioblastoma, and breast and colon carcinoma xenografts by Hsp70 depletion. Cancer Res *62*, 7139-7142.

Ohh, M., Park, C.W., Ivan, M., Hoffman, M.A., Kim, T.Y., Huang, L.E., Pavletich, N., Chau, V., and Kaelin, W.G. (2000). Ubiquitination of hypoxia-inducible factor requires direct binding to the beta-domain of the von Hippel-Lindau protein. Nat Cell Biol *2*, 423-427.

Paw, I., Carpenter, R.C., Watabe, K., Debinski, W., and Lo, H.W. (2015). Mechanisms regulating glioma invasion. Cancer Lett *362*, 1-7.

Persson, A.I., Petritsch, C., Swartling, F.J., Itsara, M., Sim, F.J., Auvergne, R., Goldenberg, D.D., Vandenberg, S.R., Nguyen, K.N., Yakovenko, S.*, et al.* (2010). Non-stem cell origin for oligodendroglioma. Cancer Cell *18*, 669-682.

Pickart, C.M., and Eddins, M.J. (2004). Ubiquitin: structures, functions, mechanisms. Biochim Biophys Acta *1695*, 55-72.

Pineda, C.T., Ramanathan, S., Fon Tacer, K., Weon, J.L., Potts, M.B., Ou, Y.H., White, M.A., and Potts, P.R. (2015). Degradation of AMPK by a cancer-specific ubiquitin ligase. Cell *160*, 715-728.

Reinstein, E., and Ciechanover, A. (2006). Narrative review: protein degradation and human diseases: the ubiquitin connection. Ann Intern Med *145*, 676-684.

694 Rubinfeld, B., Robbins, P., El-Gamil, M., Albert, I., Porfiri, E., and Polakis, P.
695 (1997). Stabilization of beta-catenin by genetic defects in melanoma cell lines.
696 Science *275*, 1790-1792.

697 Sauvageot, C.M., Weatherbee, J.L., Kesari, S., Winters, S.E., Barnes, J.,
698 Dellagatta, J., Ramakrishna, N.R., Stiles, C.D., Kung, A.L., Kieran, M.W.*, et al.*
699 (2009). Efficacy of the HSP90 inhibitor 17-AAG in human glioma cell lines and
700 tumorigenic glioma stem cells. Neuro Oncol *11*, 109-121.

701 Semenza, G.L. (2003). Targeting HIF-1 for cancer therapy. Nat Rev Cancer *3*,
702 721-732.

703 Semenza, G.L. (2004). Intratumoral hypoxia, radiation resistance, and HIF-1.
704 Cancer Cell *5*, 405-406.

705 Shen, L., Kondo, Y., Rosner, G.L., Xiao, L., Hernandez, N.S., Vilaythong, J.,
706 Houlihan, P.S., Krouse, R.S., Prasad, A.R., Einspahr, J.G.*, et al.* (2005). MGMT
707 promoter methylation and field defect in sporadic colorectal cancer. J Natl
708 Cancer Inst *97*, 1330-1338.

709 Stiles, C.D., and Rowitch, D.H. (2008). Glioma stem cells: a midterm exam.
710 Neuron *58*, 832-846.

711 Sugiarto, S., Persson, A.I., Munoz, E.G., Waldhuber, M., Lamagna, C., Andor, N.,
712 Hanecker, P., Ayers-Ringler, J., Phillips, J., Siu, J.*, et al.* (2011). Asymmetry-
713 defective oligodendrocyte progenitors are glioma precursors. Cancer Cell *20*,
714 328-340.

715 Ulrich, H.D., and Walden, H. (2010). Ubiquitin signalling in DNA replication and
716 repair. Nat Rev Mol Cell Biol *11*, 479-489.

717 Wang, S., Sdrulla, A., Johnson, J.E., Yokota, Y., and Barres, B.A. (2001). A role
718 for the helix-loop-helix protein Id2 in the control of oligodendrocyte development.
719 Neuron *29*, 603-614.

720 Weeraratna, A.T., Jiang, Y., Hostetter, G., Rosenblatt, K., Duray, P., Bittner, M.,
721 and Trent, J.M. (2002). Wnt5a signaling directly affects cell motility and invasion
722 of metastatic melanoma. Cancer Cell *1*, 279-288.

723 Yadavilli, S., Scafidi, J., Becher, O.J., Saratsis, A.M., Hiner, R.L., Kambhampati,
724 M., Mariarita, S., MacDonald, T.J., Codispoti, K.E., Magge, S.N.*, et al.* (2015).
725 The emerging role of NG2 in pediatric diffuse intrinsic pontine glioma. Oncotarget
726 *6*, 12141-12155.

727 Yuen, T.J., Silbereis, J.C., Griveau, A., Chang, S.M., Daneman, R., Fancy, S.P.,
728 Zahed, H., Maltepe, E., and Rowitch, D.H. (2014). Oligodendrocyte-encoded HIF
729 function couples postnatal myelination and white matter angiogenesis. Cell *158*,
730 383-396.

Zhu, Y., Guignard, F., Zhao, D., Liu, L., Burns, D.K., Mason, R.P., Messing, A., and Parada, L.F. (2005). Early inactivation of p53 tumor suppressor gene cooperating with NF1 loss induces malignant astrocytoma. Cancer Cell *8*, 119-130.

Zhu, Y., Tian, Y., Du, J., Hu, Z., Yang, L., Liu, J., and Gu, L. (2012). Dvl2-dependent activation of Daam1 and RhoA regulates Wnt5a-induced breast cancer cell migration. PLoS One *7*, e37823.

Zochbauer-Muller, S., Fong, K.M., Virmani, A.K., Geradts, J., Gazdar, A.F., and Minna, J.D. (2001). Aberrant promoter methylation of multiple genes in non-small cell lung cancers. Cancer Res *61*, 249-255.

Zurawel, R.H., Chiappa, S.A., Allen, C., and Raffel, C. (1998). Sporadic medulloblastomas contain oncogenic beta-catenin mutations. Cancer Res *58*, 896-899.

Figure Legends

Figure 1. Daam2 is expressed in human glioma

(A) Analysis of Daam2 RNA expression across a spectrum of cancers. Data was generated by TCGA Research Network and is publicly available (see methods). Box plots represent 5%, 25%, 50%, 75%, and 95%. Asterisk denotes tumor groups significantly higher (red) or lower (blue) as compared to corresponding non-tumor ("normal") group. P-values were generated by t-test on log-transformed data. (B) Tissue microarray showing in situ hybridization expression analysis of human Daam2 across 35 LGG (red boxes) and 40 GBM (green boxes). Blue box denotes normal human brain samples. (C) Graded pathological scoring (0-low intensity, 3-high intensity) of Daam2 expression in the samples in B; values are the percentage of LGG and GBM tumors from the tissue microarray that were assigned respective score. (D) Immunohistochemistry analysis of Daam2-LacZ expression in mouse glioma generated in $Daam2^{LacZ/+}$ mice.

Figure 2. Daam2 accelerates glioma tumorigenesis

(A-B) Cell proliferation analysis of human GBM1 and GBM2 cell lines infected with lentivirus containing Daam2 or GFP control. (C-D) Soft agar assay with GBM1 cell line infected with lentivirus containing Daam2 or GFP control, images are representative. Each of these *in vitro* experiments was performed in triplicate and replicated three times. (E-G) Representative bioluminescence imaging of mice bearing CRISPR-IUE glioma with Daam2 overexpression or control, imaged at 7 weeks of age. Imaging quantification in G is derived from 7 Daam2-overexpression and 8 control mice; *p=0.0079. (H-J) Immunohistochemistry analysis of BrdU expression from mice bearing CRISPR-IUE glioma from each experimental condition. Relative number of BrdU expressing cells is quantified in J and is derived from 6 total mice, 4 slides per mouse, from each experimental condition; ***p=0.0019. Scale bar in H is 50nm. Error bars in G and J are +/- SEM.

Figure 3. Loss of Daam2 suppresses glioma tumorigenesis

(A) qRT-PCR demonstrating effective knockdown of human Daam2 mRNA expression in human GBM1 cell line infected with lentivirus containing Daam2-shRNAi or scrambled control. (B) Cell proliferation analysis of human GBM1 cell line infected with human Daam2-shRNAi or scrambled control lentivirus. (C-E) Representative bioluminescence imaging of mice transplanted with GBM1 cell lines transfected with Daam2-shRNAi or scrambled control, imaged 6 weeks

post-transplantation. Imaging quantification is derived from 7 mice transplanted with GBM1/Daam2-shRNAi and 5 GBM1/scrambled controls; *p=0.0325. (F-H) Representative bioluminescence imaging of mice bearing CRISPR-IUE glioma generated in *Daam2+/-* or *Daam2-/-* mice, imaged at 8 weeks of age. Imaging quantification is derived from 8 *Daam2-/-* and 9 *Daam2+/-* mice; **p=0.0049. (I-K) Immunohistochemistry analysis of BrdU expression from mice bearing CRISPR-IUE glioma from each experimental condition. Relative number of BrdU expressing cells is quantified in K and is derived from 6 total mice, 4 slides per mouse, from each experimental condition; ****p=0.00001. Scale bar in I is 50nm. Error bars in E, H and K are +/- SEM.

Figure 4. Daam2 suppresses VHL expression

(A) Heatmap analysis of RPPA data showing the core cohort of proteins downregulated by overexpression of Daam2 in the PB-Ras mouse glioma model. (B) Correlation of Daam2 mRNA expression with VHL and Akt pS473 protein expression data and HIF1α mRNA expression. Protein and mRNA expression data from samples was obtained from The Cancer Proteome Atlas (TCPA) and correlations with Daam2 mRNA was performed using Pearson's. Abbreviated cancer type is listed on top panel and number of tumors analyzed in the TCPA dataset for each cancer type is listed in parenthesis; GBM is denoted by green text. (C-F) Representative immunohistochemical analysis of VHL expression in CRISPR-IUE glioma tumors derived from Daam2-overexpression (D) or knockout

of Daam2 (F) and associated controls. (G-J) Representative immunohistochemical analysis of Akt pS473 expression in CRISPR-IUE glioma tumors derived from Daam2-overexpression (H) or knockout of Daam2 (J) and associated controls. Images are representative of analysis performed on 6 independent tumors for each experimental condition. (K) Immunoblot with antibodies against HIF1α from protein lysates derived from CRISPR-IUE glioma overexpressing Daam2 or control. Scale bars in C and G are 50nm.

Figure 5. Daam2 promotes gliogenesis via suppression of VHL

(A-B) Cell proliferation analysis of human GBM1 and GBM2 cell lines infected with lentivirus containing Daam2, GFP control, or Daam2+VHL. (C-E, I) Representative bioluminescence imaging of mice bearing PB-Ras glioma with Daam2 overexpression, Daam2+VHL overexpression, or control, imaged at 10days post-natal. Imaging quantification in I is derived from 10 Daam2-overexpression, 6 Daam2+VHL, and 12 control mice; *p=0.0001, **p=0.0046. (F-H, M) Immunohistochemistry analysis of BrdU expression from mice bearing PB-Ras glioma from each experimental condition. Relative number of BrdU expressing cells is quantified in M and is derived from 6 total mice, 4 slides per mouse, from each experimental condition; *p=0.0089, **p=0.0007. (J-L) Representative immunohistochemical analysis of VHL expression in PB-Ras glioma from described experimental conditions and associated controls. (N-P) Representative immunohistochemical analysis of Akt pS473 expression in PB-Ras glioma tumors derived from the described experimental conditions and

associated controls. Images in J-P are representative of analysis performed on 6 independent tumors for each experimental condition. Statistics derived by one-way analysis of variance (ANOVA) and followed by Tukey's test for between-group comparisons. Scale bar in F is 50nm. Error bars in I and M are +/- SEM.

Figure 6. Daam2 mediates VHL degradation and ubiquitination

(A) Immunoprecipitation of Flag-Daam2, followed by immunoblot with VHL on lysates derived from PB-Ras glioma overexpressing Flag-Daam2. Detection of endogenous VHL in the "IP" lane, indicates Daam2 associates with VHL in mouse glioma. (B,D) 293 cells were transfected with VHL and Daam2 (or control). 24 hrs after transfection, cells were treated with 40μg/ml cycloheximide and incubated for the indicated time before harvest. Western blotting was performed to monitor VHL levels using anti-VHL antibody. Quantification in D shows the effect of Daam2 on VHL stability. Half-life of VHL (5.082hr) was significantly decreased in the presence of Daam2 (3.679hr). Error bars represent mean ± SEM (n=3). Half-life was determined via nonlinear, one-phase exponential decay analysis (half-life parameter, K, is significantly different in two conditions: p=0.0081). Error bars represent mean ± SEM (n=3). (C) Daam2 enhances VHL ubiquitination. 293T cells were co-transfected with Flag-VHL, HA-UB(ubiquitin), and Myc-Daam2. Cells were treated with MG132 (10ug/ml) 6 hrs before harvest. Whole-cell lysate were immunoprecipitated with anti-Flag M2 beads then analyzed by western blotting with Flag and HA antibodies.

Figure 1

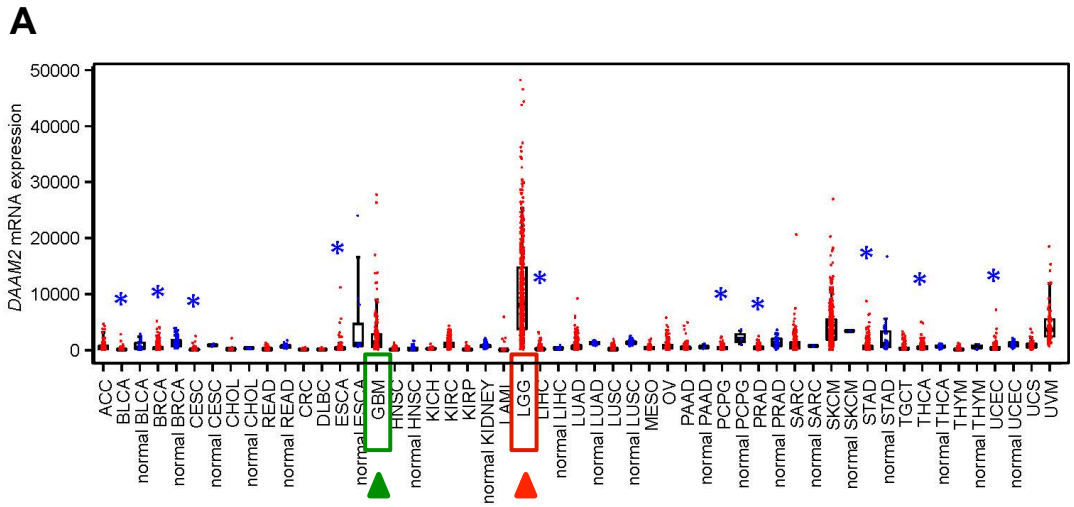

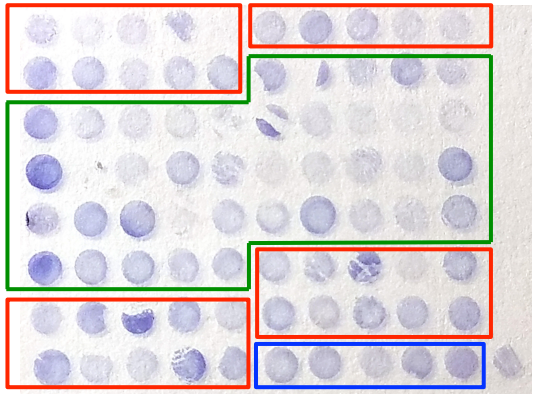

C

Score	LGG	GBM
0	8%	0%
1	15%	24%
2	62%	61%
3	23%	16%

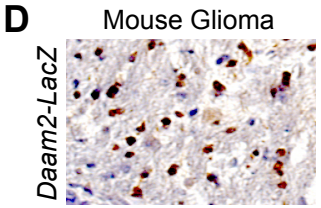

Figure 2

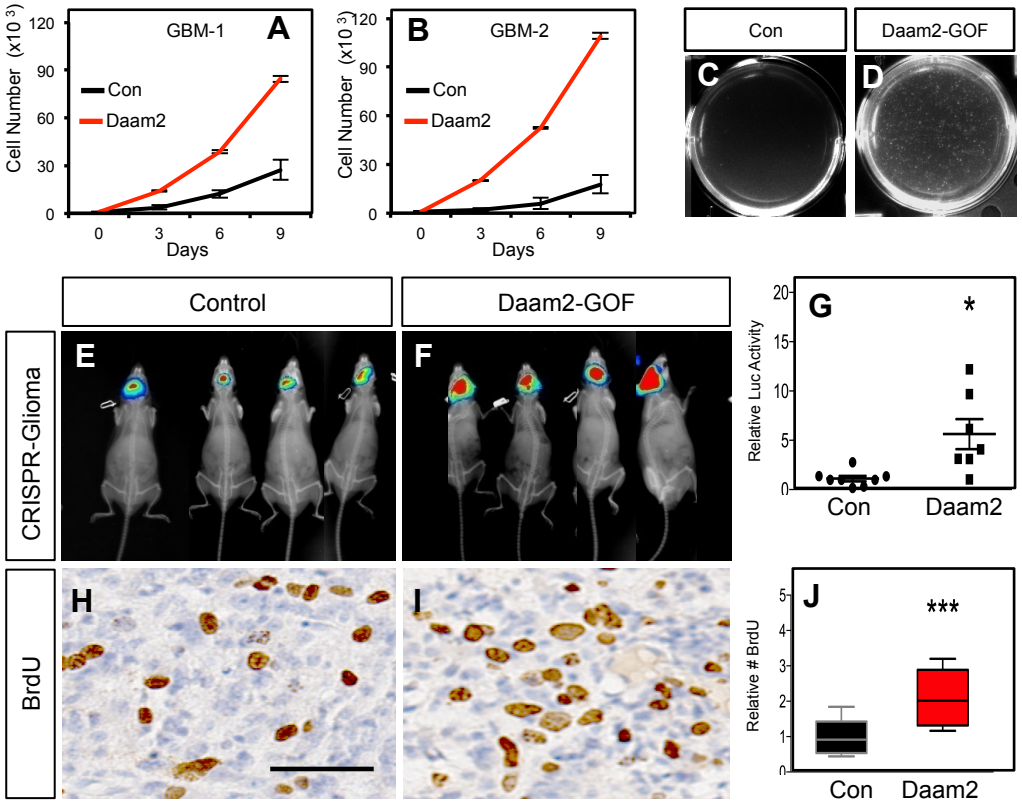
A
GBM-1
Cell Number (x10 3)
120
90
60
30
0
Con
Daam2
0
3
6
9
Days
B
GBM-2
Cell Number (x10 3)
120
90
60
30
0
Con
Daam2
0
3
6
9
Days
Con
Daam2-GOF
C
D
Control
Daam2-GOF
CRISPR-Glioma
E
F
G
*
Relative Luc Activity
20
15
10
5
0
Con
Daam2
BrdU
H
I
J
***
Relative # BrdU
5
4
3
2
1
0
Con
Daam2

Figure 3

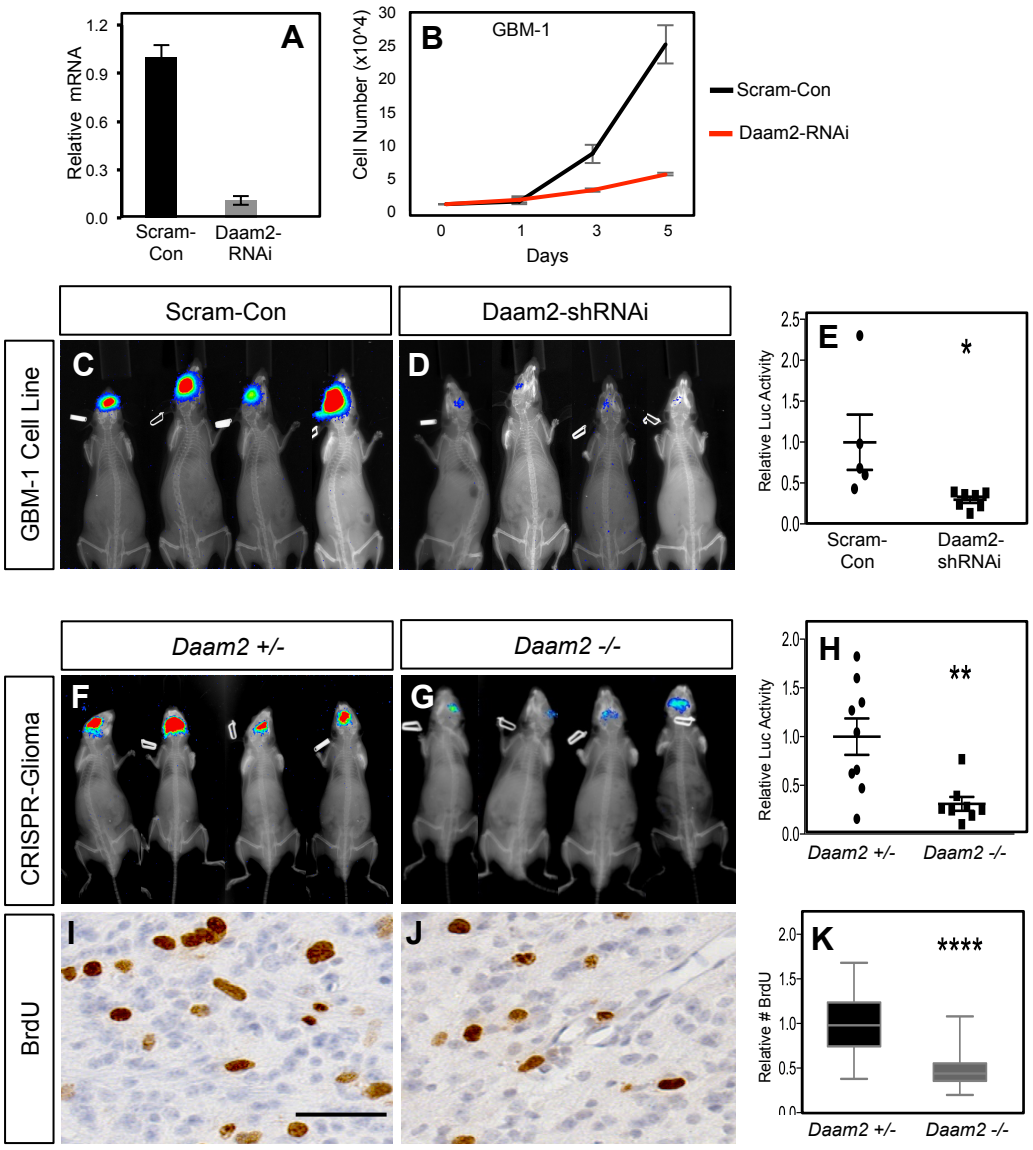
A
Relative mRNA
1.2
0.9
0.6
0.3
0.0
Scram-Con
Daam2-RNAi
B
GBM-1
Cell Number (x10^4)
30
25
20
15
10
5
0
0
1
3
5
Days
Scram-Con
Daam2-RNAi
Scram-Con
Daam2-shRNAi
GBM-1 Cell Line
C
D
E
Relative Luc Activity
2.5
2.0
1.5
1.0
0.5
0.0
*
Scram-Con
Daam2-shRNAi
Daam2 +/-
Daam2 -/-
CRISPR-Glioma
F
G
H
Relative Luc Activity
2.0
1.5
1.0
0.5
0.0
**
Daam2 +/-
Daam2 -/-
BrdU
I
J
K
Relative # BrdU
2.0
1.5
1.0
0.5
0.0
****
Daam2 +/-
Daam2 -/-

Figure 4

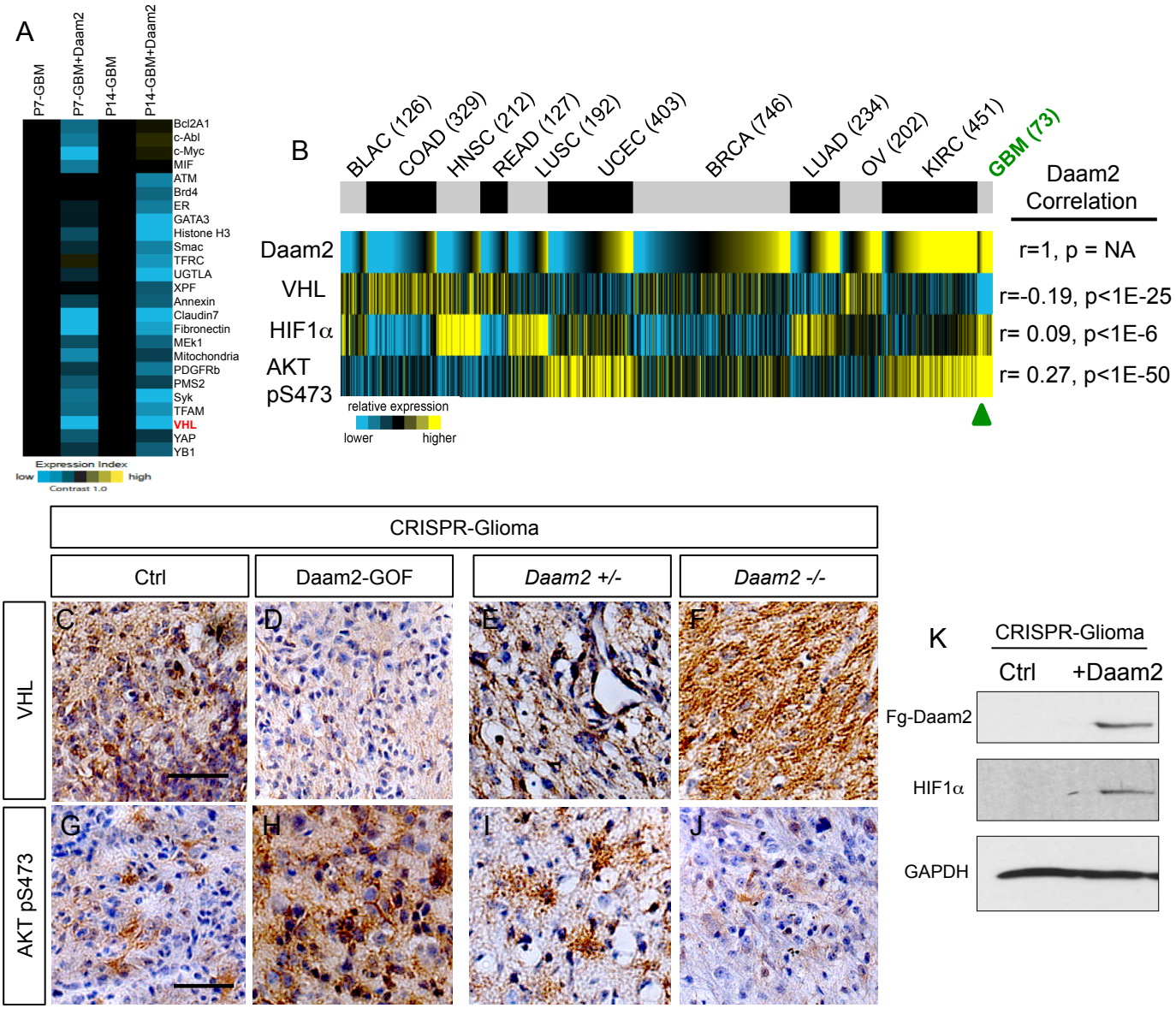
A
P7-GBM
P7-GBM+Daam2
P14-GBM
P14-GBM+Daam2
Bcl2A1
c-Abl
c-Myc
MIF
ATM
Brd4
ER
GATA3
Histone H3
Smac
TFRC
UGTLA
XPF
Annexin
Claudin7
Fibronectin
MEk1
Mitochondria
PDGFRb
PMS2
Syk
TFAM
VHL
YAP
YB1
Expression Index
low
high
Contrast 1.0
B
BLAC (126)
COAD (329)
HNSC (212)
READ (127)
LUSC (192)
UCEC (403)
BRCA (746)
LUAD (234)
OV (202)
KIRC (451)
GBM (73)
Daam2 Correlation
Daam2
VHL
HIF1α
AKT pS473
r=1, p = NA
r=-0.19, p<1E-25
r= 0.09, p<1E-6
r= 0.27, p<1E-50
relative expression
lower
higher
CRISPR-Glioma
Ctrl
Daam2-GOF
Daam2 +/-
Daam2 -/-
VHL
AKT pS473
C
D
E
F
G
H
I
J
K
CRISPR-Glioma
Ctrl
+Daam2
Fg-Daam2
HIF1α
GAPDH

Figure 5

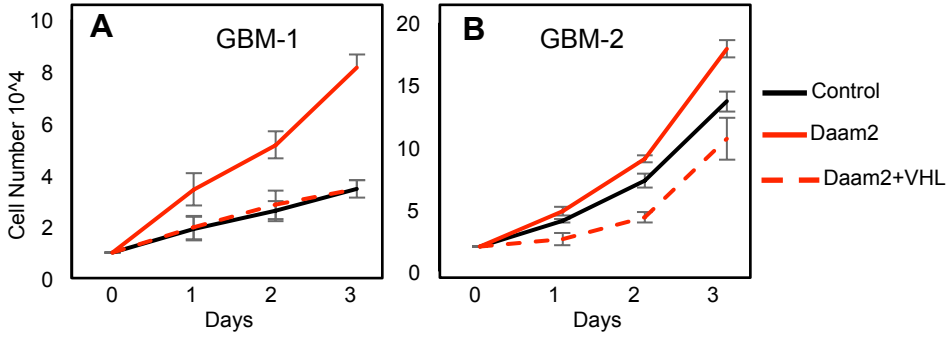
A
GBM-1
B
GBM-2
Cell Number 10^4
Days
Days
Control
Daam2
Daam2+VHL

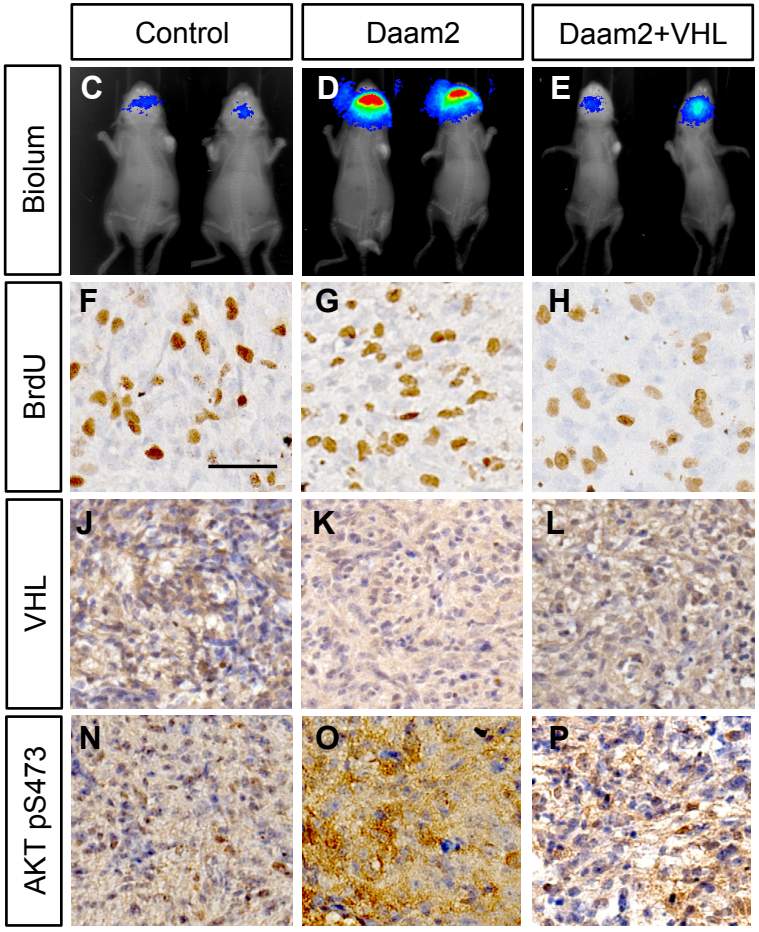
Control
Daam2
Daam2+VHL
Biolum
BrdU
VHL
AKT pS473
C
D
E
F
G
H
J
K
L
N
O
P

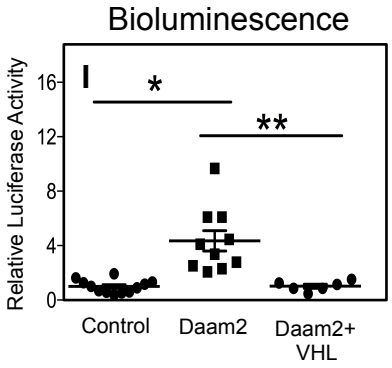
Bioluminescence
I
*
**
Relative Luciferase Activity
Control
Daam2
Daam2+ VHL

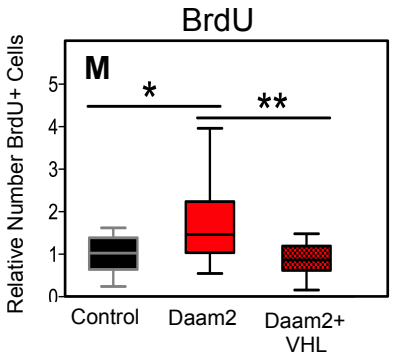
BrdU
M
*
**
Relative Number BrdU+ Cells
Control
Daam2
Daam2+ VHL

Figure 6

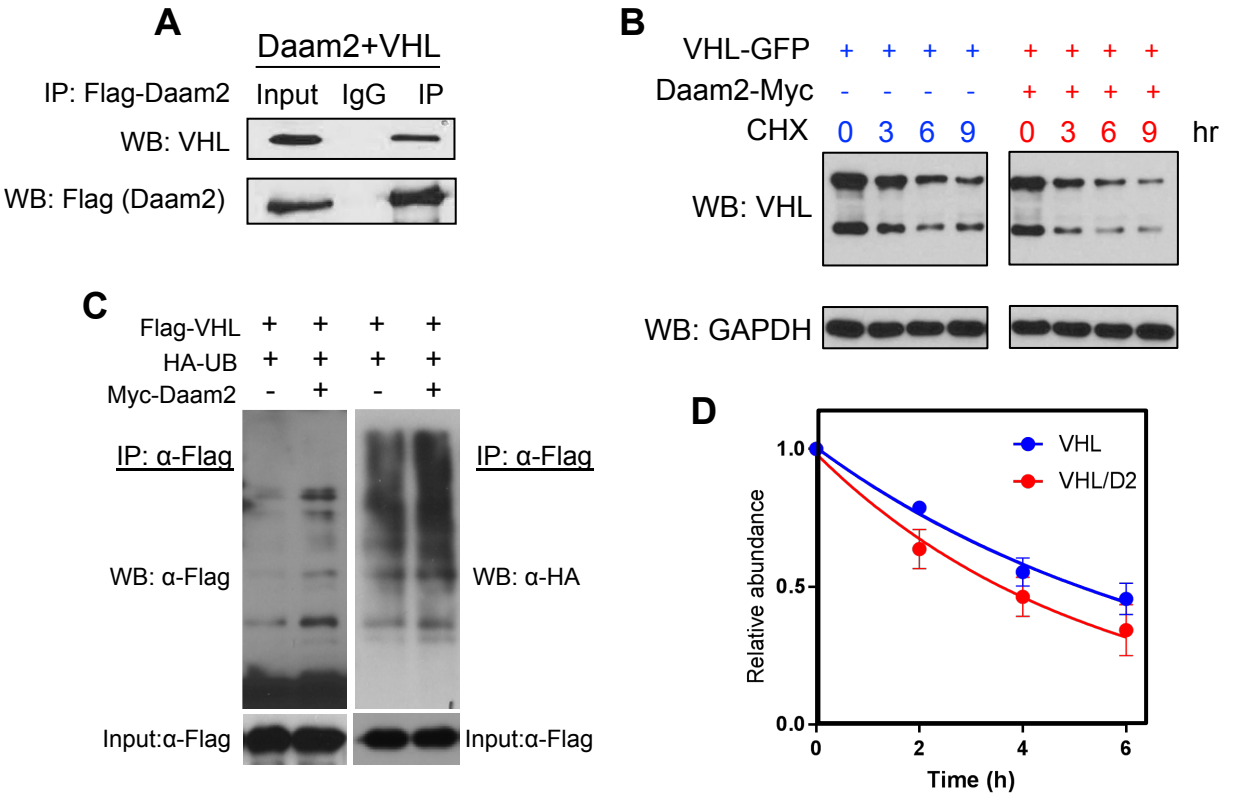
A
Daam2+VHL
IP: Flag-Daam2
Input
IgG
IP
WB: VHL
WB: Flag (Daam2)
B
VHL-GFP + + + + + + + +
Daam2-Myc - - - - + + + +
CHX 0 3 6 9 0 3 6 9 hr
WB: VHL
WB: GAPDH
C
Flag-VHL + + + +
HA-UB + + + +
Myc-Daam2 - + - +
IP: α-Flag
IP: α-Flag
WB: α-Flag
WB: α-HA
Input:α-Flag
Input:α-Flag
D
VHL
VHL/D2
Relative abundance
1.0
0.5
0.0
0
2
4
6
Time (h)